

Preparation of CeO₂ hollow spheres via a surfactant-assisted solvothermal route

Yuntao Song · Jingjing Wei · Yanzhao Yang ·
Zhijie Yang · Hongxiao Yang

Received: 3 December 2009 / Accepted: 8 April 2010 / Published online: 22 April 2010
© Springer Science+Business Media, LLC 2010

Abstract In this study, CeO₂ hollow spheres were synthesized via a facile surfactant-assisted solvothermal route. The synthesized products were characterized by X-ray diffraction, field emission scanning electron microscopy, transmission electron microscopy, selected area electron diffraction, and N₂ adsorption–desorption. Different solvent species has been demonstrated as the key factor responsible for the controlled morphologies. Furthermore, both the water and the oleic acid were crucial to the formation of CeO₂ hollow spheres. The possible formation mechanism of CeO₂ hollow spheres has been preliminary discussed.

Introduction

Recently, much attention has been paid to shape controlled nanostructures of metal oxide with unique properties because of the theoretical and technological significance [1–5]. Therefore, a wealth of synthetic approaches including thermal decomposition of complex precursor [6], hydrothermal/solvothermal treatments [7–10], and template directing [11] have been developed toward such shape-controlled nanomaterials. Among these methods, the solvothermal method has proven to be a very effective approach to prepare nanostructures of different morphologies with uniform size [12].

Fluorite-structured CeO₂ has proved to be a material of exceptional technological importance because of its unique properties and is being extensively used for preparing

heterogeneous catalysts [13], fuel cells [14], UV blocks [15], polishing materials [16], and especially in three-way catalysts [17]. Much effort has been focused on the development of synthetic approaches toward size/shape-controlled nanostructures, such as nanocubes [18, 19], nanotubes [20, 21], nanorods [22–25], nanowires [26], and so forth. In addition, remarkable progress has been made on the investigation of their controlled conversion and morphology-dependent properties. For example, Zhou et al. [21] reported the synthesis of large-cavity CeO₂ nanotubes by etching Ce(OH)₃ nanorods with H₂O₂, and the nanotubes showed highly reducible properties. Yang et al. [19] synthesized ceria nanocubes by a facile hydrothermal process using NaOH as precipitator, and the nanocubes exhibited excellent reducibility and high oxygen storage capacity owing to the higher activity of CeO₂ surface (100) than that of common surface (111). However, to the best of our knowledge, less effort has been devoted to the fabrication of CeO₂ hollow spheres [27]. In particular, the formation of CeO₂ hollow spheres involves the participation of surfactant that acts as soft template. In this article, we report for the first time the synthesis of CeO₂ hollow spheres via oleic acid (OLA)-assisted solvothermal treatment. It is worth noting here that a small quantity of water is a pivotal parameter to obtain hollow structures.

Experimental section

All chemicals of analytical grade were used as received without further purification in the synthesis process, deionized water was used throughout. For the preparation of hollow spheres, a typical procedure was as follows: 0.216 g of Ce(NO₃)₃·6H₂O and 0.2 g of NaOH were put into 18 mL of absolute ethanol, subsequently 2.0 g of OLA

Y. Song · J. Wei · Y. Yang (✉) · Z. Yang · H. Yang
School of Chemistry and Chemical Engineering, Shandong
University, Jinan, Shandong 250100, People's Republic of China
e-mail: yzhyang@sdu.edu.cn

and 1.0 mL of deionized water were added into the mixture. The resultant system was transferred into a Teflon-lined stainless steel autoclave of 25.0-mL capacity without stirring, sealed, and maintained at 180 °C for 24 h. For the synthesis of CeO₂ nanocubes, the reaction procedures were similar to those of the hollow spheres, except for the ethanol was substituted by *n*-butyl alcohol. After cooling to room temperature, the products were collected by centrifugation, and washed with ethanol several times to remove the residues. Finally, all the products were dried in an electric oven at 60 °C for 6 h.

The morphology and structure of the products were characterized using a transmission electron microscope (TEM, JEM 100-CX II) with an accelerating voltage of 100 kV, and a field-emission scanning electron microscope (FE-SEM, JEOL JSM-6700F). X-ray diffraction (XRD) patterns collected on a Japan Rigaku D/Max- γ A 200 X-ray diffractometer with Cu K α radiation ($\lambda = 1.54178 \text{ \AA}$). N₂-desorption isotherms were measured on a QuadraSorb SI apparatus at 77 K. The surface areas were calculated by the Brunauer–Emmett–Teller (BET) method, and the pore size distribution was calculated from the desorption branch using the Barrett–Joyner–Halenda (BJH) theory. Fourier transformed infrared (FT-IR) spectra were recorded on a Nicolet 5DX FT-IR spectrometer using KBr pellet technique in the range of 400–4000 cm⁻¹.

Results and discussion

The phase purity of the product was examined by the XRD pattern. Figure 1 shows the XRD patterns of the synthesized product. All the characteristic peaks can be indexed to a face-centered cubic phase [space group Fm3m (225)] of ceria (JCPDS card no. 34-0394). No diffraction peaks from impurities are found, indicating the high purity of the sample.

The size and morphology of the obtained products were further examined by TEM and SEM. A typical TEM image in Fig. 2a shows that the products consist of a large portion

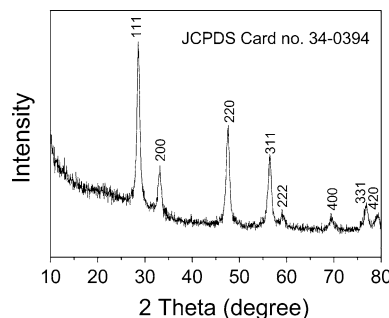


Fig. 1 XRD patterns of the as obtained hollow spheres

of spherical particles. Furthermore, the contrast difference between the light center and the dark edge of the spheres indicates the hollow nature of the spheres. The diameter of the hollow spheres was estimated to be in the range 120–180 nm, and the shell thickness was about 40 nm. The corresponding selected area electron diffraction (SAED) pattern shows typical rings, indicating its polycrystalline nature (inserted in Fig. 2a). The magnified SEM image shown in Fig. 2b exhibited detailed morphology of the obtained product, indicating the shells of the hollow spheres are composed of numerous nanocrystals with an average size of 15 nm, and the shell thickness of the hollow structures is about 40 nm, which is consistent with the TEM result. However, when *n*-butyl alcohol was employed as the solvent, a typical TEM image of the product is shown in Fig. 2c. All the particles display cubic morphology with a mean size of 50 nm, and the SEM image in Fig. 2d further confirms its cubic morphology.

To investigate the as-obtained products with varied morphologies in more detail, different alcohols with various carbon numbers (C_nH_{2n+1}-OH, *n* = 2–6) were employed as the solvent. The experimental results showed that the solvent had a remarkable influence on the morphology of the product. As can be seen from the TEM image in Fig. 3a, CeO₂ hollow spheres could also be obtained when *n*-C₃H₇OH was used as the solvent, and the size of the product is in the range 140–180 nm. As in the case of alcohols such as *n*-C₅H₁₁OH or *n*-C₆H₁₃OH, nanocubes were obtained as the main product (Fig. 3b, c). It can be explained that, in the reaction system, the solvent consists of both alcohol and water (1 mL). When either C₂H₅-OH or *n*-C₃H₇-OH was employed as the solvent, it can be miscible with water to form a homogeneous system. However, the other alcohols cannot be miscible with the water, thus a liquid–liquid interface occurs. Therefore, we can speculate that a homogeneous system is indispensable for the formation of hollow structures.

To further understand the formation mechanism of the hollow structure, a series of controlled experiment were carried out. The effect of the different water content on the morphology of the product was investigated by TEM. It was found that the water content was the key factor responsible for the controlled morphology of the CeO₂. When the experiment was carried out in the absence of water, some random nanoparticles but no hollow spheres were obtained as the single product (shown in Fig. 4a). Interestingly, when 0.5 mL of water was introduced into the system, as shown in Fig. 4b, some hollow spheres appeared, the proportion of the hollow spheres was estimated to be 40%, and the size of the spheres was in a broad range of 50–300 nm. Increasing the water volume to 0.8 mL, formation of CeO₂ hollow spheres had significantly enhanced, and the ratio of the hollow spheres was

Fig. 2 TEM (a) and SEM (b) images of as-obtained hollow spheres, inset in (a) is the corresponding SAED pattern of the hollow spheres; TEM (c) and SEM (d) images of the nanocubes

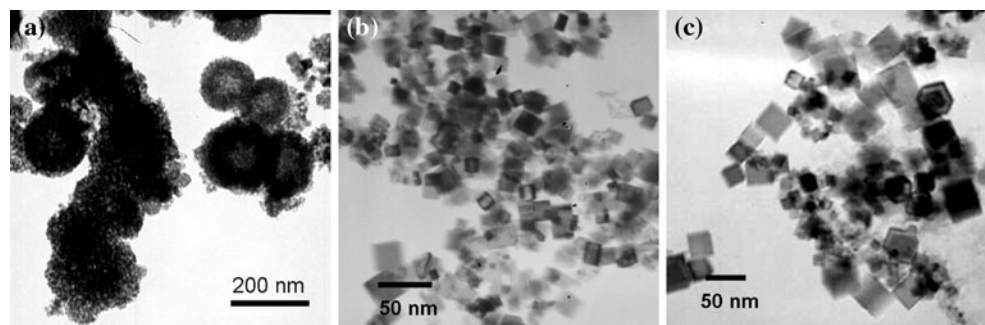
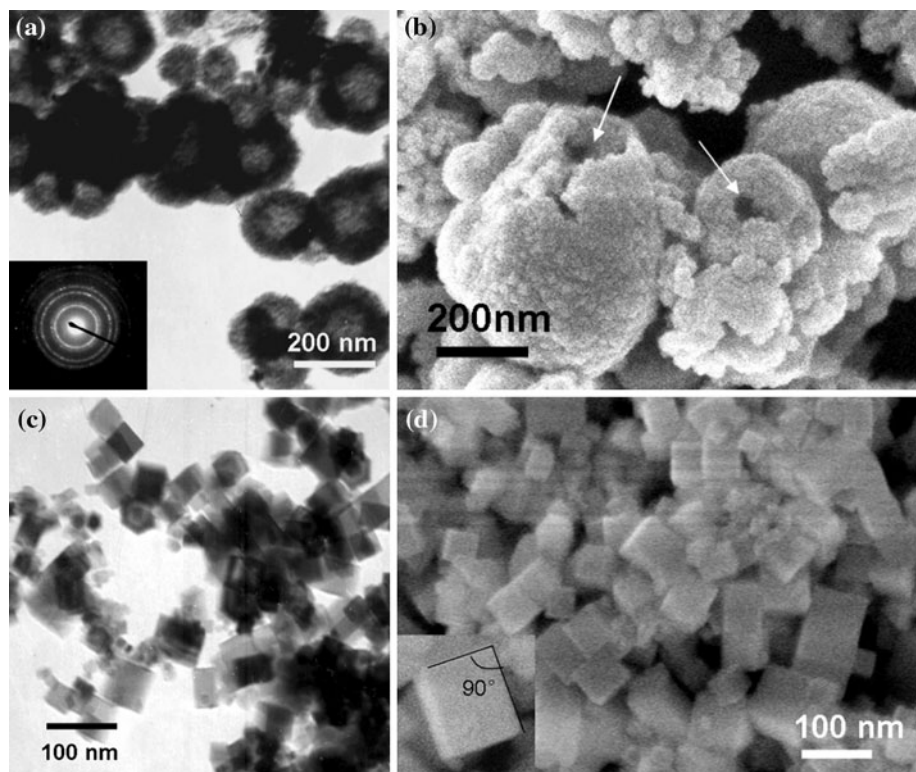


Fig. 3 TEM images of products obtained with different alcohols: **a** $n\text{-C}_3\text{H}_7\text{OH}$, **b** $n\text{-C}_5\text{H}_{11}\text{OH}$, **c** $n\text{-C}_6\text{H}_{13}\text{OH}$

about 80%, as can be seen in Fig. 4c. However, further increasing the water volume to 2 mL, the products were mainly random nanoparticles. Besides, the role of the OLA was also investigated. When the experiment was carried out without the addition of OLA, hollow spheres were not further observed and agglomerated nanoparticles were obtained as the sole product in Fig. 4d. Based on the above-experimental results, the formation mechanism of CeO_2 hollow spheres was proposed as follows: in the solvothermal reaction system, ethanol can be miscible with water to form a homogeneous liquid phase. Subsequently OL anions may self-assemble to form micelles due to the amphiphilic nature of OL anions, and a small quantity of water would transform to surface hydroxyls at elevated temperature, which is similar to the previous report on the

fabrication of Co_3O_4 hollow spheres [8]. The surface hydroxyls acted as binders, making the nanocrystals tend to aggregate. In order to further investigate whether there was an interaction between OLA and newly formed CeO_2 nanocrystals, the FT-IR spectra was recorded as shown in Fig. 5, the product exhibits absorption bands in the region $2800\text{--}2900\text{ cm}^{-1}$, attributed to the C-H stretching mode of hydrocarbons, and the bands at 1454 and 1544 cm^{-1} are assigned to the stretching mode of COO^- . These results suggested that the interaction between the nanocrystals and OLA occurred, which cannot be destroyed through ethanol washing. This result can also explain that when 2 mL or more water was introduced into the system, the excess amount of water may disturb the structure of the soft template.

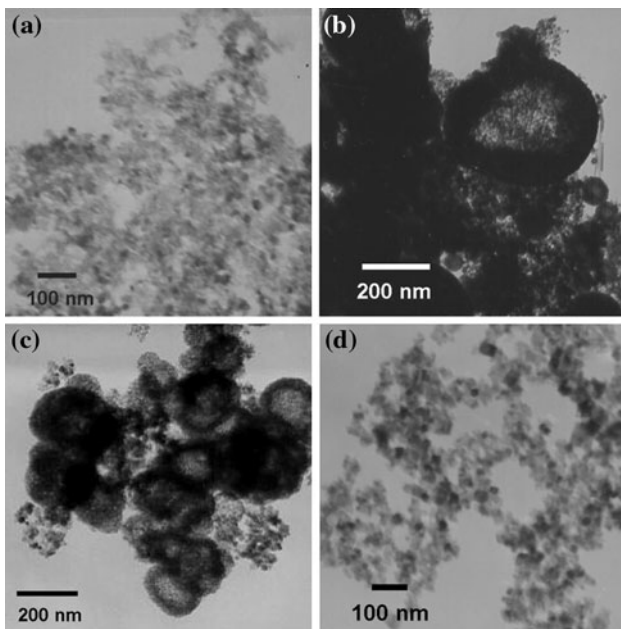


Fig. 4 TEM images of water content experiment: **a** 0 mL, **b** 0.5 mL, **c** 0.8 mL, **d** is obtained in the absence of OLA

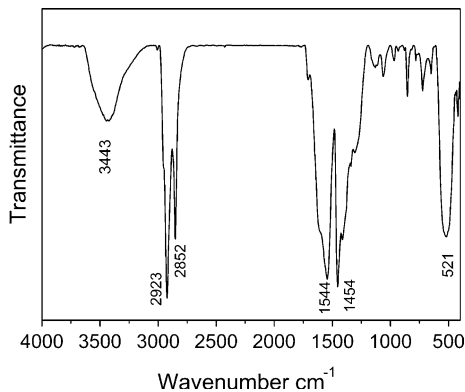


Fig. 5 FT-IR spectrum of as-obtained CeO_2 hollow spheres

As can be seen in the FESEM image of an individual broken sphere (Fig. 2b), the surface roughness was due to the aggregation of CeO_2 nanoparticles, leading to the porous structure. The porous nature of the product was further investigated by N_2 adsorption–desorption. The N_2 adsorption–desorption isotherm of the hollow spheres shown in Fig. 6 exhibits a hysteresis loop in the relative pressure range of 0.3–1.0, indicating the presence of the mesopores, which are formed through the aggregation of the nanocrystals. The corresponding pore size distribution curve (inserted in Fig. 6) displays a pore size distribution from 4 to 23 nm, centered at ca. 6.0 nm. The calculated pore volume is $0.235 \text{ cm}^3/\text{g}$ and the specific surface area is $83.2 \text{ m}^2/\text{g}$. This high surface area may be favorable for achieving better performance in redox catalysis.

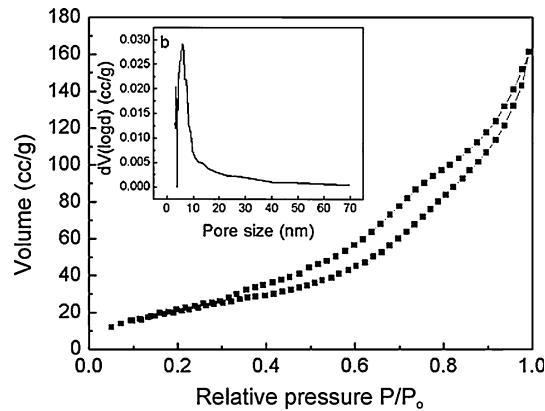
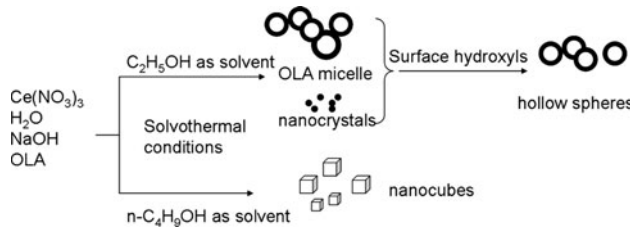


Fig. 6 N_2 adsorption–desorption isotherm of CeO_2 hollow spheres, and inset is the corresponding BJH pore size distribution curve



Scheme 1 Schematic illustration of the possible formation process for hollow spheres and nanocubes of CeO_2

Based on the above experiments, we speculate that the formation of CeO_2 hollow spheres may due to the self assembly of newly formed nanocrystals with the assistance of OLA and water. Herein, the OLA may act as surfactant to form micelles in the homogeneous system at elevated temperature. When $n\text{-C}_m\text{H}_{2m+1}\text{OH}$ ($m \geq 4$) is applied as the solvent, an interface of the mixture occurs at room temperature. A slight change of the particle size can be observed, which can be attributed to the effects of the solvent. It should be mentioned that the variation in the particle size may result from the Ostwald ripening. The detailed formation mechanism of nanocubes needs to be further investigated. The whole process can be depicted as in Scheme 1.

Conclusion

In summary, a facile OLA-assisted solvothermal process could be used to fabricate CeO_2 hollow spheres. Hollow spheres were formed when ethanol was employed as solvent, and nanocubes were formed when ethanol was replaced by *n*-butyl alcohol. The detailed formation mechanism of hollow structure was briefly discussed. This one-pot solution chemistry may offer a facile route to fabricate other inorganic materials. Furthermore, the hollow structure

of CeO₂ may be favorable for achieving better performance in catalysis.

Acknowledgement This work was supported by the Natural Science Foundation of China (Grant 20876089) and Key Technologies R&D Program of China (Grant 2007BAD87B05).

References

1. Ould-Ely T, Prieto-Centurion D, Kumar A, Guo W et al (2006) *Chem Mater* 18:1821
2. Pinna N, Niederberger M (2008) *Angew Chem Int Ed* 47:5292
3. An KL, Lee N, Park J, Kim SC, Hwang Y (2006) *J Am Chem Soc* 128:9753
4. Yin S, Akita SG, Shinozaki M et al (2008) *J Mater Sci* 43:2234. doi:[10.1007/s10853-007-2070-3](https://doi.org/10.1007/s10853-007-2070-3)
5. Qiao H, Zheng Z, Zhang LZ et al (2008) *J Mater Sci* 43:2778. doi:[10.1007/s10853-008-2510-8](https://doi.org/10.1007/s10853-008-2510-8)
6. Park J, An KJ, Hwang YS, Park J-G et al (2004) *Nat Mater* 3:891
7. Wang SB, Min YL, Yu SH (2007) *J Phys Chem C* 111:3551
8. He T, Chen DR, Jiao XL (2004) *Chem Mater* 16:737
9. Yan CL, Zou LJ, Xue DF et al (2008) *J Mater Sci* 43:2263. doi:[10.1007/s10853-007-2072-1](https://doi.org/10.1007/s10853-007-2072-1)
10. Li F, Qin QH, Wu JF et al (2010) *J Mater Sci* 45:348. doi:[10.1007/s10853-009-3942-5](https://doi.org/10.1007/s10853-009-3942-5)
11. Wang X, Peng Q, Li YD (2007) *Acc Chem Res* 40:635
12. Xu XX, Wei W, Qiu XM (2006) *Nanotechnology* 17:3416
13. Murugan B, Ramaswamy AV (2007) *J Am Chem Soc* 129:3062
14. Yahiro HY, Baba K, Eguchi H, Arai J (1988) *Electrochim Soc* 135:2077
15. Yabe S, Yamashita M, Momose S, Tahira K et al (2001) *Int J Inorg Mater* 3:1003
16. Feng XD, Sayle DC, Wang ZL, Paras MS et al (2006) *Science* 312:1504
17. Granados ML, Galisteo FC, Lambrou PS, Mariscal R et al (2006) *J Catal* 239:410
18. Yang SW, Gao L (2006) *J Am Chem Soc* 128:9330
19. Yang ZQ, Zhou KB, Liu XW, Tian Q, Lu DY, Yang S (2007) *Nanotechnology* 18:185606
20. Han WQ, Wu LJ, Zhu YM (2005) *J Am Chem Soc* 127:12814
21. Zhou KB, Yang ZQ, Yang S (2007) *Chem Mater* 19:1215
22. Zhang DS, Fu HX, Shi LY, Pan CS et al (2007) *Inorg Chem* 46:2446
23. Mai HX, Sun LD, Zhang YW, Si R et al (2005) *J Phys Chem B* 109:24380
24. Chen GZ, Sun SX, Song XY, Yin ZL et al (2007) *J Mater Sci* 42:6977. doi:[10.1007/s10853-006-1254-6](https://doi.org/10.1007/s10853-006-1254-6)
25. Devaraju MK, Yin S, Sato T (2009) *Appl Mater Interfaces* 1:2694
26. Tang B, Zhuo LH, Ge JC, Wang GL et al (2005) *Chem Comm* 3565
27. Titirici M-M, Antonietti M, Thomas A (2006) *Chem Mater* 18:3808